ISSN:2790-1688 Volume-14-(2025)

Influence of Layer Angle and Fiber Type on the Impact Resistance of Composite Laminates

Lingwei Hu*

The College of Aeronautics, Nanjing University of Aeronautics and Astronautics, Nanjing, China.

m19871826699@163.com

Abstract. As modern science and technology progress rapidly, composite materials are increasingly applied in aerospace, weapon manufacturing, sports equipment, and construction due to their high strength and toughness. This study employs Abaqus software to develop a finite element model of a hemispherical bullet impacting a fiber-reinforced composite laminate. The simulation results are validated against experimental data from the literature, confirming the model's reliability. The research investigates the relationship between the initial and residual velocities of the laminate after impact, considering different bullet speeds, layer angles, and hybrid configurations. The findings indicate that for laminates with varying layer angles, when the bullet's initial speed exceeds 350 m/s, the residual speed post-impact shows a roughly linear correlation with the initial speed. Within the range of 200-350 m/s, the layer angle significantly influences the residual speed after penetration, with [0°/45°] layered laminates demonstrating the highest ballistic limit. For laminates with different hybrid configurations, optimizing the ratio of carbon to kevlar fibers, positioning low-strength materials on the impact side, high-strength materials on the back side, and concentrating similar materials can substantially enhance the impact resistance of composite laminates.

Keywords: Composite laminates; layer angle; hybrid configuration; impact resistance.

1. Introduction

Fiber-reinforced composites (FRP) emerged in the mid-20th century, driven by the demands of the aerospace industry. Known for their lightweight nature, high strength, corrosion resistance, and design flexibility, these materials have rapidly expanded into various sectors, including automotive, construction, sports equipment, and military applications[1]. Research on fiber-reinforced composites focuses on continuously optimizing material properties, such as enhancing strength, improving toughness, and increasing impact resistance and protective capabilities[2]. The layering structure and type of fiber materials significantly affect the impact resistance of laminates. Therefore, a comprehensive investigation of these two factors can provide valuable insights for the design of composite laminates, facilitating the optimization of their structure and material properties to enhance impact resistance.

Firstly, the layering structure influences the energy absorption density, damage modes, and overall stiffness of laminates during impact. For instance, Wu et al.[3] investigated the impact performance of glass fiber-reinforced composite laminates with and without embedded wire mesh through experimental methods. The results indicated that embedding wire mesh enhances impact resistance, with the effect becoming more pronounced as the wire diameter increases and spacing decreases. Zheng[4] conducted impact tests on fiber or metal hybrid laminates without foam cores, analyzing how layering affects damage. The findings showed that adding wire mesh to fiber or metal hybrid laminates significantly improved tensile strength, impact resistance, and energy absorption. Ge[5] developed a finite element model for thick woven carbon fiber composite laminates under impact loads to study the influence of spiral structures on impact resistance. The results revealed that spiral composite laminates exhibited higher peak forces and lower energy absorption capabilities. Zhao et al.[6] constructed a layered embedded wire mesh spiral composite-metal hybrid structure and analyzed its damage and energy absorption characteristics under impact loads. Their findings indicated that including wire mesh significantly increased energy absorption uniformity, enhancing material utilization. Li[7] explored the effects of laminate thickness on the mechanical behavior of carbon fiber laminates under impact loads through simulation and experimental analysis. The results

indicated that increasing laminate thickness improved energy absorption, although fracture displacement exhibited a decreasing trend. Jia et al.[8] simulated impact tests with a model to investigate how thickness ratio affects the ballistic limit and damage modes of laminates, shedding light on the failure mechanisms of composites. The results showed that for a fixed thickness of fiber laminates, reducing the carbon fiber layer thickness ratio slightly decreased the energy absorption and areal density, with minimal changes in average areal density and ballistic limit. Ren[9] studied the influence of foam core density on the impact resistance of core structures with different fiber laying methods. The results revealed that the damage area in a [0°/90°] panel was largely unaffected by core density, while the damage area in a [0°/+45°/90°/-45°] panel decreased with increasing core density. Huang Lingmin [10] examined the effects of layer angle on the impact response of composite laminates under impact conditions through experimental and numerical methods. The findings indicated that as the layer angle increased, the failure mechanism shifted from large-scale matrix damage at the specimen edges due to in-plane relative motion to severe fiber fracture in the impact area caused by bending deformation. Additionally, the hybridization of different fiber types and layering sequences also affects the impact resistance of laminates. For instance, Sun et al.[11] studied the high-speed impact behavior of composite plates with varying hybrid ratios through experiments and numerical simulations, finding that increasing the volume fraction of kevlar fibers generally raised the critical penetration speed. Zhao[12] utilized Abaqus finite element simulation software to model the impact of projectiles on Kevlar fiber or ceramic interlayer composite armor, obtaining various results by altering the hybrid ratio of fibers. The optimal range for the proportion of mixed fibers was found to be between 0.3 and 0.7, arranged in an alternating pattern. Cui[13] prepared six hybrid fiber laminates with different ratios of carbon and glass fibers and compared their impact performance through ballistic impact tests. The results indicated that as the proportion of carbon fibers in the laminate increased, the ballistic limit gradually decreased. Silva et al.[14] investigated the impact response of glass or kevlar or epoxy laminates under ballistic conditions, finding that hybridizing kevlar composites with glass improved the impact absorption capacity of rigid composite armor. Luo[15] studied the impact performance of carbon-kevlar fiber hybrid composites through experimental methods, revealing that laminates containing kevlar fibers exhibited superior impact resistance, enhancing the damage tolerance of carbon fiber composites. He[16] researched the impact performance of polyimide fiber or carbon fiber hybrid composites through experimental methods. The results demonstrated that the presence of polyimide fibers effectively improved the impact resistance of carbon fiber laminates. Elias et al.[17] explored the effects of different layering sequences on the impact performance of laminates composed of various fibers and epoxy resin through experiments, concluding that using glass fibers for the first layer was more effective than using Kevlar fibers; a combination of carbon and glass in the center layer was most effective, while using carbon fibers in the final layer was not recommended. Ju et al.[18] studied the influence of layering sequences of carbon and glass fibers on the impact resistance of composites through experiments, finding that uniform spacing of carbon and glass fibers within layers most effectively enhanced performance, improving it by approximately 60% compared to pure glass fiber reinforcement, although the enhancement effect diminished with an increasing number of intervening layers.

Despite extensive research conducted by scholars both domestically and internationally on the impact resistance of composite laminates, as well as on ceramic and metal composite structures, several critical issues remain inadequately addressed. For instance, studies on impact performance often assume a fixed layering angle, with limited investigation into how varying layering angles affect the impact resistance of composite laminates. Therefore, it is essential to examine the impact performance of laminates at different layering angles. Furthermore, most research employs a single type of material for laminates, and the potential effects of layering two or more types of composites (such as carbon fiber, kevlar fiber, and glass fiber) on impact performance have not been thoroughly explored. To address these gaps, this study will utilize Abaqus/Explicit finite element analysis software to investigate two key areas. First, it will assess the ballistic protection performance of

composite laminates at various layering angles, analyzing bullet speed loss and the failure characteristics of the laminates to provide insights for performance optimization. Second, the research will explore the ballistic performance of laminates created by optimally combining carbon fibers, glass fibers, and kevlar fibers, identifying the similarities and differences in their impact resistance to offer new perspectives for composite design.

2. Establishment and Validation of the Finite Element Model

In developing the finite element model for the impact of projectiles on carbon fiber composite laminate structures, this chapter primarily employs the various modules of the commercial finite element software ABAQUS/Explicit. This includes tasks such as geometry modeling, assignment of material properties, and the configuration of interactions and boundary conditions. Building on this foundation, the chapter reproduces similar simulations and experimental results from existing literature to validate the robustness of the finite element modeling approach utilized in this study.

2.1 Geometric Model

2.1.1 Establishment of the Geometric Models for the Laminate and Penetrating Projectile

The geometric models of the carbon fiber composite laminate and the hybrid fiber composite laminate developed in this chapter are presented in Figures 2-1 and 2-3, respectively. For clarity, a single layer of carbon fiber is designated as C, a single layer of glass fiber as G, and a single layer of kevlar fiber as K. To optimize computational efficiency and leverage the model's symmetry, only a quarter of the model has been constructed. The laminate structure is a square layer measuring 300 mm × 300 mm. In the finite element model shown in Figure 1, each laminate has a thickness of 0.5 mm, consisting of a total of 12 layers of carbon fiber, resulting in an overall thickness of 6 mm. The layering configurations include five arrangements: [0°/90°], [45°/-45°], [0°/45°/90°/-45°], [0°/45°], and [60°/-60°], as illustrated in the Figure 2.

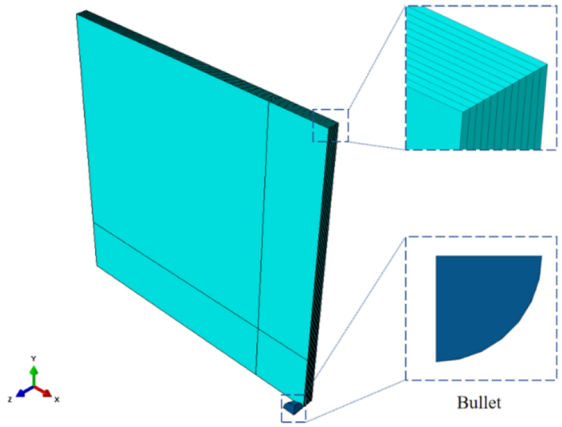

Figure 1. Geometric Structure of the Carbon Fiber Composite Laminate

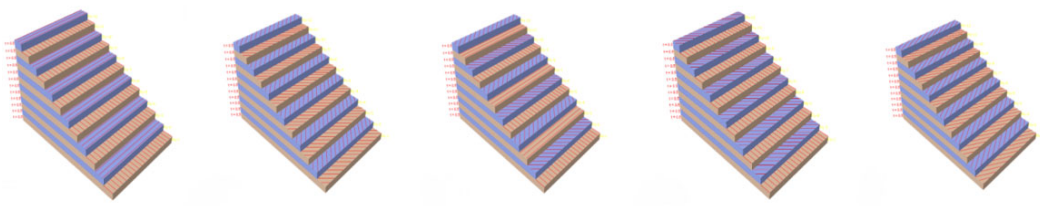

Figure 2. Layering Configurations at Different Angles

In the finite element model presented in Figure 3, the fundamental structure remains consistent with that of Figure 1-1. However, the materials of the laminate, in the order facing the projectile, consist of 4 layers of carbon fiber (C), 4 layers of glass fiber (G), and 4 layers of kevlar fiber (K),

collectively referred to as $C_4G_4K_4$, with a total thickness of 6 mm. The investigation into hybrid configurations is categorized into several groups: the control group ($C_4G_4K_4$), proportional groups ($C_6G_3K_3$, $C_3G_6K_3$, $C_3G_3K_6$), sequential groups ($G_4C_4K_4$, $K_4G_4C_4$), and dispersed groups ($[CGK]_4$, $[CCGGKK]_2$), as illustrated in Figure 4.

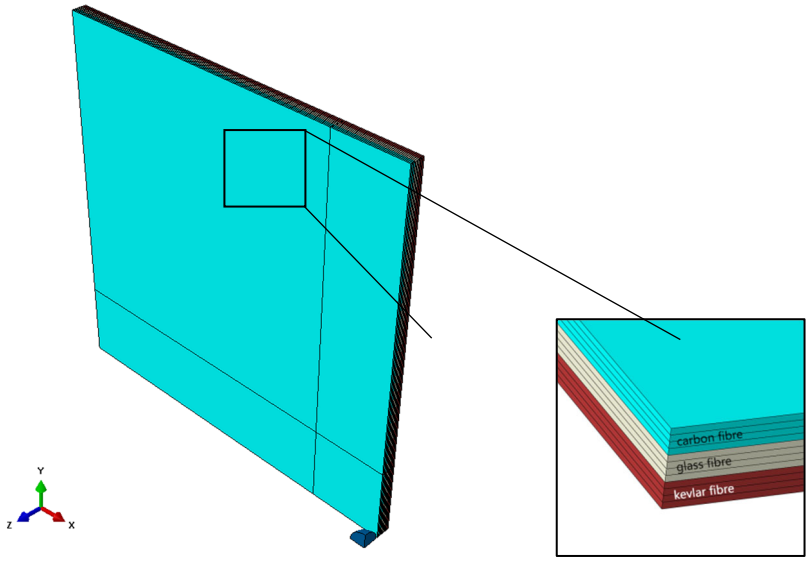

Figure 3. Geometric Structure of the Hybrid Fiber Composite Laminate (e.g. C4G4K4)

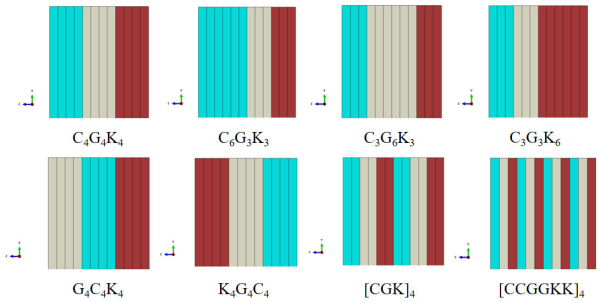

Figure 4. Schematic of Different Hybrid Laminate Layering Configurations

At the same time, a 12.7 mm armor-piercing projectile will strike the center of the laminate structure perpendicularly along the normal to its outer surface. In the finite element model, the armor-piercing projectile illustrated in Figure 2-1 has been simplified to a hemispherical shape with a radius of 6.35 mm for the purposes of analysis and calculation.

2.1.2 Mesh Division of the Laminate and Armor-Piercing Projectile Models

In the predefined field, a speed is applied to the projectile in the Z direction, while velocities in the other directions are set to 0. To achieve a balance between accuracy and computation time, a dense mesh is created only for the central area of the laminate and the region in contact with the projectile, with a coarser mesh used elsewhere. For the laminate, a three-dimensional solid homogeneous 8-node mesh element (C_3D_8R) is employed, as shown in Figure 5(a), resulting in a total of 97,200 mesh elements for the CFRP. The projectile is represented using three-dimensional average tetrahedral mesh elements ($C_3D_{10}M$), illustrated in Figure 5(b), which comprises a total of 3,696 mesh elements.

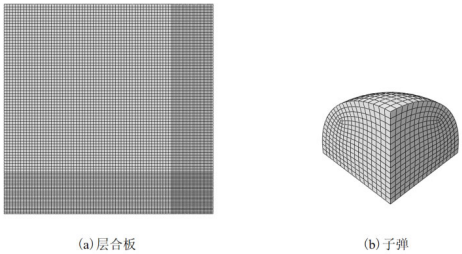

Figure 5. Mesh Division Models of the Laminate and Projectile

2.2 Material Properties

The projectile is composed of Q235 steel, with a mass of approximately 4.2 g, a density of 7.85 g/cm³, an elastic modulus of 210 GPa, and a Poisson's ratio of 0.3. The mechanical behavior of the C, G, and K laminates is described using an orthotropic constitutive model, where the relationship between stress (σ) and strain (ε) is expressed as follows:

$$\boldsymbol{\sigma} = \begin{bmatrix} \sigma_1 \\ \sigma_2 \\ \sigma_3 \\ \sigma_{12} \\ \sigma_{23} \\ \sigma_{13} \end{bmatrix} = \begin{bmatrix} C_{11} & C_{12} & C_{13} & 0 & 0 & 0 \\ & C_{22} & C_{23} & 0 & 0 & 0 \\ & & C_{33} & 0 & 0 & 0 \\ & & & C_{44} & 0 & 0 \\ & & & & C_{55} & 0 \\ & & & & & C_{66} \end{bmatrix} \begin{bmatrix} \varepsilon_1 \\ \varepsilon_2 \\ \varepsilon_3 \\ \varepsilon_{12} \\ \varepsilon_{23} \\ \varepsilon_{13} \end{bmatrix} = \boldsymbol{C\varepsilon} \quad (1)$$

In the equation, C_{ij} (i, j =1, 2, ..., 6) represents the stiffness coefficients, which are also the elements of the stiffness matrix *C*. Their expressions are as follows:

$$\begin{cases} C_{11} = \frac{1-v_{23}v_{32}}{E_2E_3\Delta}, C_{22} = \frac{1-v_{13}v_{31}}{E_1E_3\Delta}, C_{33} = \frac{1-v_{12}v_{21}}{E_1E_2\Delta} \\ C_{12} = \frac{v_{12}+v_{32}v_{13}}{E_1E_3\Delta}, C_{23} = \frac{v_{23}+v_{21}v_{13}}{E_1E_2\Delta}, C_{23} = \frac{v_{13}+v_{12}v_{23}}{E_1E_2\Delta} \\ C_{44} = G_{12}, C_{55} = G_{23}, C_{66} = G_{13} \\ \Delta = \frac{1-v_{12}v_{21}-v_{23}v_{32}-v_{31}v_{13}-2v_{21}v_{32}v_{13}}{E_1E_2E_3} \end{cases} \quad (2)$$

In the equation, E_i (i = 1, 2, 3) represents the elastic modulus in the *i* direction. G_{ij} (i,j = 1, 2, 3; $i \neq j$) denotes the shear modulus in the *i-j* plane. v_{ij} (i,j = 1, 2, 3; $i \neq j$) indicates the Poisson's ratio in the *i-j* plane.

It is evident that the orthotropic model necessitates the definition of nine independent elastic material constants. The damage and failure behavior of CFRP laminates under impact loading is quite complex. Therefore, this study utilizes the three-dimensional Hashin failure criterion to evaluate the damage and failure conditions of the FRP laminates. The Hashin failure criterion primarily encompasses fiber tensile failure, fiber compressive failure, matrix tensile failure, and matrix compressive failure, with their respective criteria defined as follows:

(1) **Fiber Tensile Failure** ($\sigma_1 > 0$)

$$\left(\frac{\sigma_1}{X_T}\right)^2 + \left(\frac{\tau_{12}}{S_{12}}\right)^2 + \left(\frac{\tau_{13}}{S_{13}}\right)^2 = 1 \quad (3)$$

In this equation, X_t represents longitudinal tensile strength, S_{12} represents shear strength in the 1-2 plane, and S_{13} represents shear strength in the 1-3 plane.

(2) Fiber Compressive Failure ($\sigma_1 < 0$)

$$\left(\frac{\sigma_1}{X_c}\right)^2 = 1 \quad (4)$$

Here, X_c stands for longitudinal tensile strength.

(3) Matrix Tensile Failure ($\sigma_2 + \sigma_3 > 0$)

$$\left(\frac{\sigma_2+\sigma_3}{Y_t}\right)^2 + \frac{\tau_{23}^2-\sigma_2\sigma_3}{S_{23}^2} + \left(\frac{\tau_{12}}{S_{12}}\right)^2 + \left(\frac{\tau_{13}}{S_{13}}\right)^2 = 1 \quad (5)$$

Y_t represents transverse tensile strength and S_{23} represents shear strength in the 2-3 plane.

(4) Matrix Compressive Failure ($\sigma_2 + \sigma_3 < 0$)

$$\left[\left(\frac{Y_c}{2S_{23}}\right)^2 - 1\right]\left(\frac{\sigma_2+\sigma_3}{Y_c}\right) + \left(\frac{\sigma_2+\sigma_3}{2S_{23}}\right)^2 + \frac{\tau_{23}^2-\sigma_2\sigma_3}{S_{23}^2} + \left(\frac{\tau_{12}}{S_{12}}\right)^2 + \left(\frac{\tau_{13}}{S_{13}}\right)^2 = 1 \quad (6)$$

Y_c stands for Transverse compressive strength.

To implement the aforementioned constitutive models and failure criteria in the finite element model, this chapter incorporates a VUMAT user subroutine written in Fortran within Abaqus software, as illustrated in the flowchart in Figure 6.

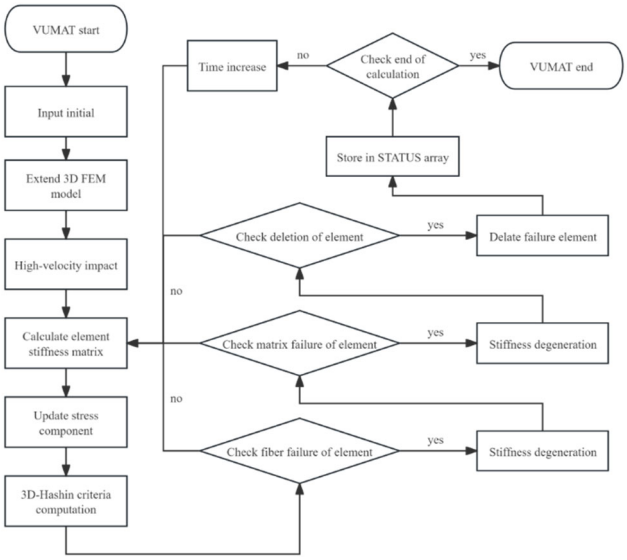

Figure 6. Flowchart of the VUMAT User Subroutine

The elastic constants and strength parameters for the Hashin failure criterion are derived from the results presented in reference [19], as detailed in Table 1.

Table 1. Elastic Constants of C, G, K and Strength Parameters for the Hashin Failure Criterion

Parameter	E_1	E_2	E_3	v_{12}	v_{13}	v_{23}	G_{12}	G_{13}	G_{23}
C	53.7	53.7	11.7	0.31	0.33	0.33	20.7	4	4
G	23.1	23.1	6.87	0.15	0.2	0.25	4.0	1.8	1.8
K	21.0	21.0	4.6	0.34	0.14	0.14	1.3	1.3	1.3
Unit of Measurement	GPa	GPa	GPa	-	-	-	GPa	GPa	GPa
Parameter	X_t	X_c	Y_t	Y_c	Z_t	Z_c	S_{12}	S_{13}	S_{23}
C	565	420	565	420	49.5	220	200	200	200
G	442	337	442	337	75	400	40	45	45
K	800	200	800	200	80	225	77	100	100
Unit of Measurement	MPa	MPa	MPa	MPa	MPa	MPa	MPa	MPa	MPa

2.3 Model Validation

To validate the reliability of the finite element modeling method described above, this chapter reproduces similar experimental results from references [20] and [21].

Using the parameters from reference [20], a finite element model was developed to simulate the impact of a flat-nosed projectile on a composite laminate. The model analyzed impacts at initial velocities of 200 m/s, 220 m/s, 240 m/s, and 260 m/s on a laminate composed of five layers, each 1 mm thick. The resulting residual velocities for these four speed groups were 96.1 m/s, 125.1 m/s, 140.6 m/s, and 171.1 m/s, while the corresponding residual velocities reported in the literature were 92.3 m/s, 124.1 m/s, 145.2 m/s, and 175.8 m/s. A bar chart comparing the simulated residual velocities with those from the literature is presented in Figure 7. The validation results demonstrate that, for the same initial velocities, the residual velocities obtained from this simulation differ from those reported in the literature by less than 5%.

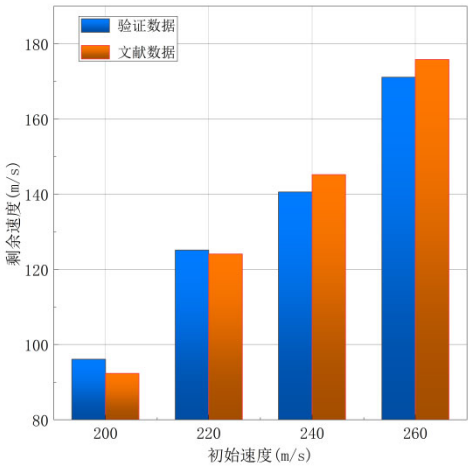

Figure 7. Comparison of Simulated Residual Velocities with Literature Values

Using the parameters from the experiments in reference [21], a finite element model was developed to simulate the impact of a flat-nosed projectile on a hybrid fiber composite laminate. The model analyzed impacts at initial velocities of 125 m/s, 138 m/s, and 150 m/s on a laminate consisting of 12 layers of hybrid fibers, with carbon fiber, glass fiber, and kevlar fiber layers having thicknesses of 0.55 mm, 0.25 mm, and 0.20 mm, respectively, arranged in a [0°, 90°] layup. The residual velocities obtained from the model validation were 50.2 m/s, 70.5 m/s, and 109.3 m/s, while the corresponding values reported in the literature were 61.4 m/s, 82.5 m/s, and 101.8 m/s. During the impact process, the target plate initially experienced shear failure due to the compressive load from the projectile, resulting in a bullet hole. As the projectile penetrated the target plate, some of its kinetic energy was absorbed, leading to a decrease in projectile speed and a corresponding reduction in the impact load until it reached the tensile capacity of the fiber yarns. Subsequently, the target plate underwent tensile deformation until the fibers stretched and ultimately broke, allowing the projectile to pass through the plate while carrying a plug (marked by a red circle in Figure 8). This process closely resembles the impact behavior observed in the experiments reported in reference [21].

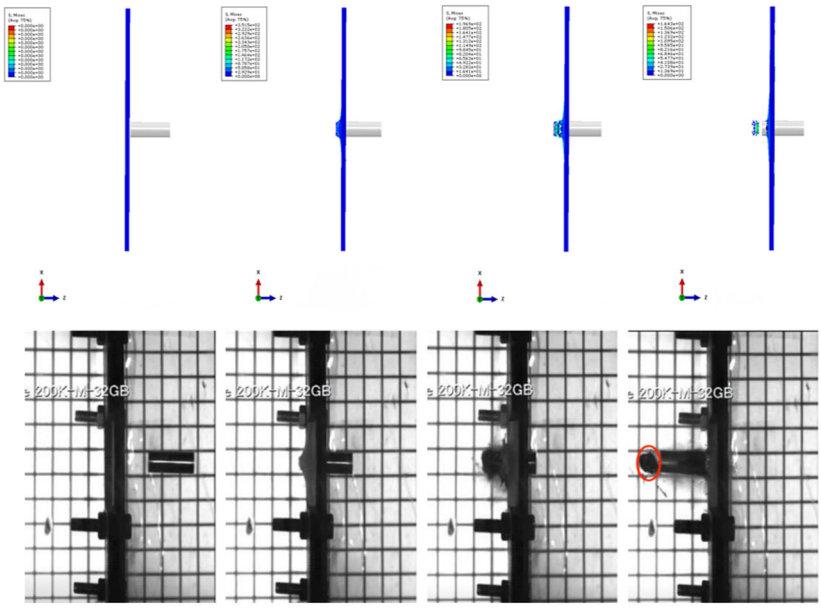

Figure 8. Comparison of Projectile Impact Processes in Model Validation and Experiments from Reference [21]

In conclusion, the finite element model developed in this study is accurate, and the analysis methodology is reliable. Thus, it is appropriate for performing finite element analyses of the impact resistance of carbon fiber laminates with different layer angles and fiber types.

3. Finite Element Results Analysis

3.1 Influence of Layer Angle on the Impact Resistance of Laminates

When examining the effect of layer angle, the relationship between the initial speed and the residual speed of the projectile is illustrated in Figure 9(a). For initial speeds of 350 m/s or higher, the layer angle has minimal impact on the projectile's residual speed. As shown in Figure 10(a), at an initial speed of 350 m/s, the residual velocities across five different layer angles are quite similar. Furthermore, within this speed range, there is a roughly linear relationship between the projectile's residual speed and its initial speed. This behavior can be attributed to the fact that impacts at speeds of 350 m/s or greater are classified as high-speed, and laminates generally exhibit weak resistance to such impacts; therefore, the layer configuration does not significantly influence the projectile's residual speed.

In contrast, when the projectile impacts the laminate at initial speeds ranging from 200 to 350 m/s, Figure 10(b) reveals that at an initial speed of 200 m/s, the residual velocities for the five layer angles vary considerably. The layer angle has a significant effect on the residual speed after the projectile penetrates the laminate. Analyzing the ballistic limit, data for different layer angles can be derived by fitting the curve in Figure 9(a) using the least-squares method, as shown in Table 2-1. The findings indicate that the [0°/45°] layer configuration has the highest ballistic limit, approximately 200 m/s, followed by the [0°/45°/90°/-45°] configuration with a critical speed of about 170 m/s, while the [45°/-45°] configuration exhibits the lowest critical speed of approximately 158.8 m/s. From the perspective of energy absorption, the [0°/45°/90°/-45°] configuration demonstrates the best energy absorption performance, as illustrated in Figure 11. When the projectile penetrates the laminate at the same speed, the stress distribution in this configuration is more dispersed compared to the other four configurations, resulting in higher energy absorption efficiency.

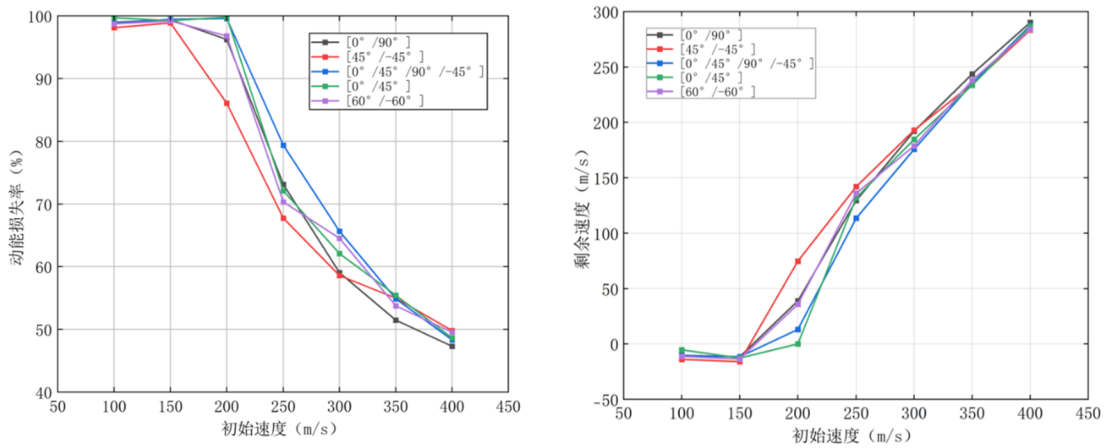

(a) 剩余速度-初始速度 (b) 子弹动能损失率-初始速度

Figure 9. (a) Projectile Residual Speed-Initial Speed Curve & (b) Kinetic Energy Loss Rate-Initial Speed Curve at Five Different Layer Angles

Table 2. Ballistic Limits at Different Layer Angles

Layer Method	[0,90]	[45/-45]	[0/45/90/-45]	[0/45]	[60/-60]
Ballistic Limit (m/s)	161.5	158.8	170.0	200.0	163.7

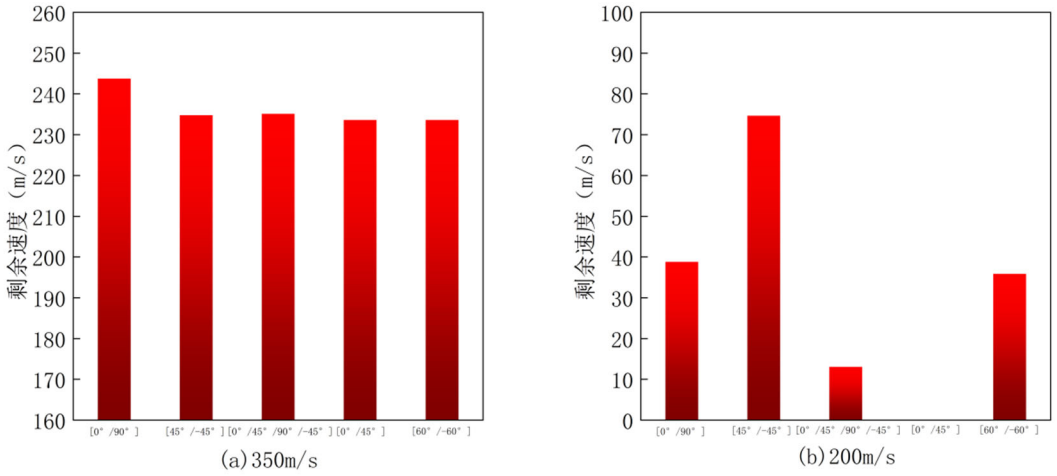

Figure 10. Projectile Residual Velocities at Five Layer Angles for Initial Speeds of 350 m/s (a) and 200 m/s (b)

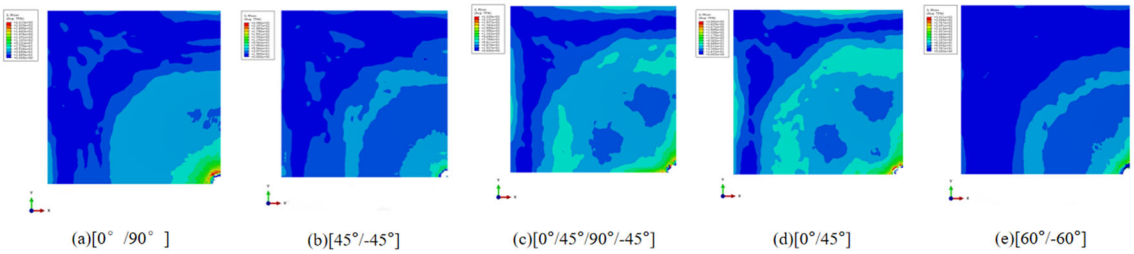

Figure 11. Damage Stress Contours for Five Layer Angles After Projectile Impact at 200 m/s

3.2 Influence of Different Hybridization Methods on the Impact Resistance of Laminates

In examining the impact of hybridization methods, the laminate layer angle was maintained at [0°/45°]. The simulation data for projectiles impacting laminates with various hybridization methods is presented in Table 3. Using the least-squares method for curve fitting, the ballistic limits for these laminates were determined and are displayed in Table 4.

Table 3. Simulation Data for Projectile Impacts on Laminates with Different Hybridization Methods

Types of Laminate	Initial Speed(m/s)	Residual Speed(m/s)	Bullet Status	Types of Laminate	Initial Speed(m/s)	Residual Speed(m/s)	Bullet Status
$C_4G_4K_4$ (Control)	120	-13.11	Rebounded	$C_6G_3K_3$ (Proportional)	120	-10.13	Rebounded
	130	-11.18	Rebounded		130	-12.06	Rebounded
	140	0	Embedded		140	-13.22	Rebounded
	150	45.77	Penetrated		150	31.87	Penetrated
	160	66.41	Penetrated		160	56.52	Penetrated
$C_3G_6K_3$ (Proportional)	100	-11.31	Rebounded	$C_3G_3K_6$ (Proportional)	120	-9.95	Rebounded
	110	-12.16	Rebounded		130	0	Embedded
	120	6.97	Penetrated		140	0	Embedded
	130	34.96	Penetrated		150	5.59	Penetrated

	140	52.43	Penetrated		160	31.96	Penetrated
$G_4C_4K_4$ (Sequential)	120	-10.36	Rebounded	$K_4G_4C_4$ (Sequential)	120	-10.36	Rebounded
	130	0	Embedded		130	0	Embedded
	140	0	Embedded		140	0	Embedded
	150	0	Embedded		150	33.91	Penetrated
	160	50.90	Penetrated		160	50.90	Penetrated
$[CGK]_4$ (Dispersed)	110	-7.61	Rebounded	$[CCGGKK]_2$ (Dispersed)	110	-14.84	Rebounded
	120	0	Embedded		120	0	Embedded
	130	11.20	Penetrated		130	0	Embedded
	140	44.73	Penetrated		140	38.06	Penetrated
	150	54.92	Penetrated		150	58.49	Penetrated

Table 4. Ballistic Limits (m/s) for Laminates with Different Hybridization Methods

Hybridization Method	$C_4G_4K_4$	$C_6G_3K_3$	$C_3G_6K_3$	$C_3G_3K_6$	$G_4C_4K_4$	$K_4G_4C_4$	$[CGK]_4$	$[CCGGKK]_2$
Ballistic Limit (m/s)	140	143.1	116.0	140.0	150.0	140.0	120.0	130.0

From Tables 2-3, it is evident that the ballistic limit for the control group $C_4G_4K_4$ is approximately 140 m/s. For the proportional group, the ballistic limit of $C_6G_3K_3$ is about 143.1 m/s, representing a year-on-year increase of 2.2%. This indicates that increasing the proportion of carbon fiber in the laminate enhances its ballistic limit. Additionally, under the same initial speed, the residual speed of the projectile after impact is lower than that of the control group, demonstrating improved energy absorption performance of the laminate. This enhancement is attributed to the strong compressive strength and higher elastic modulus of carbon fiber, which effectively withstands projectile impacts. In contrast, the ballistic limit for $C_3G_6K_3$ is approximately 116 m/s, reflecting a year-on-year decrease of 17.1% compared to the control group. This suggests that increasing the proportion of glass fiber in the laminate does not improve its impact resistance. The ballistic limit for $C_3G_3K_6$ is around 140 m/s, similar to that of the control group. However, under the same initial speed, the projectile's residual speed after penetrating the laminate is lower than that of $C_6G_3K_3$. This indicates that increasing the proportion of kevlar fiber in the laminate effectively enhances energy absorption. The improved performance is due to the high tensile strength of kevlar fiber, which undergoes significant deformation upon impact, allowing it to effectively absorb projectile energy.

In the sequential group, the ballistic limit for $G_4C_4K_4$ is the highest, at about 150 m/s, reflecting a year-on-year increase of 7.1%. This enhancement can be attributed to the compressive strength of glass fiber, which significantly reduces the projectile's speed upon initial impact. The projectile then strikes the carbon fiber layer, which has greater compressive strength, followed by the kevlar fiber layer, known for its high tensile and compressive strength. Overall, the laminate's strength increases progressively with each layer, indicating that using glass fiber as the strike face and kevlar fiber as the backing face improves the laminate's impact resistance. The ballistic limit of $K_4G_4C_4$ is approximately 140 m/s, similar to that of the control group. However, under the same initial speed, the projectile's residual speed after penetrating the laminate is lower than that for $C_4G_4K_4$, suggesting superior energy absorption capabilities of this laminate. This phenomenon arises because kevlar fiber

can effectively impede projectile motion through significant deformation. As shown in the comparison of damage stress contours in Figure 12, placing kevlar fiber in the first layer prevents it from fully utilizing its deformation advantages. Nevertheless, due to its relatively high compressive and tensile strength, kevlar fiber still contributes to maintaining a certain level of impact resistance.

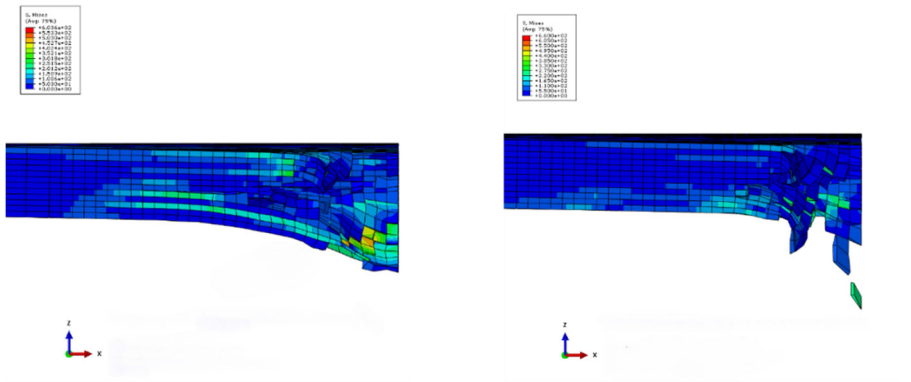

Figure 12. Comparison of Impact Damage Between Control Group C4G4K4 and Sequential Group $K_4G_4C_4$

In the dispersed groups, the ballistic limits for $[CGK]_4$ and $[CCGGKK]_2$ are approximately 120 m/s and 130 m/s, respectively, reflecting decreases of 14.3% and 7.1% compared to the control group. This suggests that when similar materials are arranged more concentrically, the impact resistance of the laminate improves. This enhancement occurs because a concentrated arrangement allows the materials to better utilize their strength characteristics, while a dispersed layout effectively weakens the material's impact resistance.

In summary, increasing the proportions of carbon fiber and kevlar fiber in the laminate, placing glass fiber on the strike face, positioning kevlar fiber on the backing face, and arranging similar materials concentrically can significantly enhance the impact resistance of composite laminates.

4. Conclusions

(1) For composite laminates with varying layer angles, when the projectile's initial speed exceeds 350 m/s, the layer angle has little effect on the projectile's residual speed. In this case, the residual speed after impact shows a roughly linear relationship with the initial speed. However, when the initial speed is between 200 and 350 m/s, the layer angle significantly influences the residual speed after penetration. Notably, the laminate with a [0°/45°] layer angle exhibits the highest ballistic limit, indicating that this configuration provides superior ballistic performance compared to the other four layer angles. Thus, the [0°/45°] laminate demonstrates the best impact resistance.

(2) Regarding laminates with different material proportions, increasing the ratios of carbon fiber and kevlar fiber enhances the laminate's impact resistance, while increasing the proportion of glass fiber reduces it. When considering different material layer sequences, placing glass fiber on the strike face and kevlar fiber on the backing face, where low-strength materials are positioned to absorb the impact and high-strength materials are on the opposite side, effectively improves the laminate's impact resistance. Additionally, for laminates with dispersed arrangements, the impact resistance increases as the arrangement of identical materials becomes more concentrated. Overall, appropriately increasing the proportions of carbon fiber and kevlar fiber, positioning low-strength materials on the strike face, placing high-strength materials on the backing face, and arranging similar materials concentrically can significantly enhance the impact resistance of composite laminates.

References

[1] Li Kaiqiang, Yang Jinshuai, Qian Lei. Analysis of the Mechanical Properties and Construction Techniques of Carbon Fiber Reinforced Composites in Building Structures. *Jushe*, 2025, (10): 44-46.

[2] Zhang Weijun, Xue Zhongmin, Wang Xin, et al. Typical Applications and Future Prospects of Fiber Reinforced Composites. *Journal of Composite Materials Science and Engineering*, 2024, (S1): 30-37. DOI: 10.19936/j.cnki.2096-8000.20241201.006.

[3] Wu Y., You P., Hua W., et al. Experimental Investigation on the Damage Mechanism of GFRP Laminates Embedded with/without Steel Wire Mesh under Low-Velocity Impact and Post-Impact Tensile Loading. *e-Polymers*, 2024, 24(1).

[4] Zheng Zhiqiu. Research on the Impact Resistance of Fiber Reinforced Metal Hybrid Laminates. *East China Jiaotong University*, 2020. DOI: 10.27147/d.cnki.ghdju.2020.000617.

[5] Ge Xinxin. Study on Low-Velocity Impact Damage and Residual Compressive Strength of Diagonal Weave Carbon Fiber Laminates. *Huazhong University of Science and Technology*, 2022. DOI: 10.27157/d.cnki.ghzku.2022.002603.

[6] Zhao Zheji, Li Xiaobin, Li Zhi, et al. Study on the Impact Resistance of Spiral FRP/Metal Hybrid Structures. *Journal of Wuhan University of Technology (Transportation Science & Engineering)*, 1-10 [2024-09-06]. http://kns.cnki.net/kcms/detail/42.1824.u.20240409.1323.060.html.

[7] Li Huanyu. Study on the Bending and Impact Mechanical Properties of Carbon Fiber Composite Laminates. *Beijing University of Chemical Technology*, 2024. DOI: 10.26939/d.cnki.gbhgu.2024.000493.

[8] Jia Yuankun. Research on the Impact Resistance of Carbon/Aramid Hybrid Fiber Composites. *Civil Aviation University of China*, 2022. DOI: 10.000484.

[9] Ren Tianyu. Damage Analysis of Composite Foam Sandwich Panels under Impact. *Taiyuan University of Technology*, 2022. DOI: 10.27352/d.cnki.gylgu.2022.001731.

[10] Huang Lingmin. Numerical and Experimental Study on the Impact Performance of 2D Bi-Axial Weave Composites at Off-Axis Angles. *Zhejiang University of Technology*, 2022. DOI: 10.27786/d.cnki.gzjlg.2022.000634.

[11] Sun J., Wang C., Zhao S., et al. High-Velocity Impact Resistance and Energy Absorption Behavior of Carbon-Kevlar Hybrid Composite Laminates. *Polymer Composites*, 2024, 45(1): 847-861.

[12] Zhao Wei. Design and Numerical Simulation Study of Interlayer Hybrid Composite Systems and Their Impact Resistance. *Harbin Institute of Technology*, 2012.

[13] Cui Hongli. Research on the Impact Characteristics of Fiber Interlayer Hybrid Composites. *Civil Aviation University of China*, 2023. DOI: 10.27627/d.cnki.gzmhy.2023.000503.

[14] Silva D., Xavier A. A., Scazzosi, et al. High-Velocity Impact Behavior of Aramid/S2-Glass Interply Hybrid Laminates. *Applied Composite Materials*, 2021, 28: 1899-1917.

[15] Luo Ziwei. Research on the Impact Resistance and Damage Identification of Hybrid Fiber Reinforced Composites. *Guangzhou University*, 2023. DOI: 10.27040/d.cnki.ggzdu.2023.001224.

[16] He Bin. Study on the Mechanical Properties of Polyimide Fiber/Carbon Fiber Hybrid Reinforced Epoxy Resin Composites. *Beijing University of Chemical Technology*, 2020.

[17] Elias R., Rizal Z., Dayang L. M., et al. The Effects of Stacking Sequence Layers of Hybrid Composite Materials on Energy Absorption under High Velocity Ballistic Impact Conditions: An Experimental Investigation. *Journal of Material Science & Engineering*, 2013, 02(04): 1-8.

[18] Ju Luyan, Lin Haohan, Li Wei, et al. The Impact of Carbon/Glass Hybrid Fiber Layer Sequence on the Mechanical Properties of Composites. *Weapon Material Science and Engineering*, 2024.

[19] Xin Shihong. Numerical Simulation Study on the Penetration Resistance of Fiber Reinforced Resin Matrix Composite Laminates. *University of Science and Technology of China*, 2015.

[20] Wang Yuanbo, Wang Xiaojun, Hu Xiuzhang, et al. Study on the Ballistic Performance of Kevlar Laminates. *Engineering Mechanics*, 2005, (03): 76-81.

[21] Liu Yating. Research on the Impact Resistance of Carbon/Glass/Aramid Fiber Hybrid Laminates. *Civil Aviation University of China*, 2022. DOI: 10.27627/d.cnki.gzmhy.2022.000733.